CMLS, Cell. Mol. Life Sci. 60 (2003) 999–1006
1420-682X/03/050999-08
DOI 10.1007/s00018-003-3105-9

CMLS Cellular and Molecular Life Sciences

Research Article

Nicotinoprotein (NAD^+-containing) alcohol dehydrogenase: structural relationships and functional interpretations

A. Norin [a], S. R. Piersma [b,c] J. A. Duine [b] and H. Jörnvall [a,*]

[a] Department of Medical Biochemistry and Biophysics, Karolinska Institutet, 171 77 Stockholm (Sweden), Fax: + 46 8 337462, e-mail: hans.jornvall@mbb.ki.se
[b] Department of Microbiology and Enzymology, Delft University of Technology, 2628 BC Delft (The Netherlands)
[c] Present address: FOM-Institute for Atomic and Molecular Physics (AMOLF), 1098 SJ Amsterdam (The Netherlands)

Received 17 March 2003; accepted 19 March 2003

Abstract. The primary structure of nicotinoprotein alcohol dehydrogenase (ADH) from *Amycolatopsis methanolica* was determined and used for modelling against known ADH structures, and for evaluation of the coenzyme binding. The results establish the medium-chain dehydrogenase/reductase nature of the nicotinoprotein ADH. Its subunit model and that of the human class Iβ ADH subunit structure are similar, with mean α carbon deviations of 0.95 Å, but they differ in seven loops. Nicotinoprotein ADH occupies a phylogenetic position intermediate between the dimeric and tetrameric ADH families. Two of the differing loops are important for coenzyme binding in the nicotinoprotein model, where one (with a Thr271Arg exchange towards the traditional enzyme) may suggest a slight rotation of the coenzyme adenine ring in the nicotinoprotein, and the other, with an Asn288 insertion, may suggest an extra hydrogen bond to its nicotinamide ribose, favouring stronger binding of the coenzyme. Combined with previous data, this suggests differences in the details of the tight coenzyme binding in different nicotinoproteins, but a common mode for this binding by loop differences.

Key words. Nicotinoprotein; alcohol dehydrogenase; coenzyme binding; molecular modelling; loop differences; molecular evolution.

Alcohol dehydrogenases (ADHs) are common in nature. At least six protein families have given rise to enzymes with this activity [1, 2]. Two of these belong to the superfamily of 'medium-chain dehydrogenases/reductases' (MDRs) and include 'dimeric ADH' (liver ADHs) and 'tetrameric ADH' (most yeast ADHs). Both work with a zinc ion at the active site [3]. A third is represented by the insect enzyme of the short-chain dehydrogenases/reductase (SDR) super-family, working without metal [4]. Remaining forms are ADH activities in aldo-keto reductases [5], long-chain dehydrogenases/reductases [6] and iron-dependent enzymes [7].

Bacteria often have special ADH forms [8]. One such MDR form in Gram-positive bacteria, characterized from *Amycolatopsis methanolica*, has a mycothiol adduct with formaldehyde as substrate, and phylogenetically occupies a distinct position [9]. The same bacterial species also has a 'nicotinoprotein ADH', with a tightly bound coenzyme that is not dissociated from the enzyme between the reaction cycles as in classical ADHs but, instead, is regenerated by a second substrate or electron carrier [8, 10].
This nicotinoprotein ADH has been reported to be related to the liver ADHs and the mycothiol ADHs, based on partial [8] or quoted [11, 12] sequence data. It is therefore likely to be an MDR enzyme. However, its nicotinoprotein nature has not been molecularly defined and structural data have not been given. Instead, other nicotinopro-

* Corresponding author.

tein structures have been reported and appear to be different. A UDP-galactose 4-epimerase from *Escherichia coli* is a nicotinoprotein of another protein family, SDR [13], and a *Zymomonas mobilis* glucose-fructose oxidoreductase is also a different nicotinoprotein [14], while a *Pseudomonas putida* formaldehyde dehydrogenase, although an MDR nicotinoprotein, has a special loop explaining the tight coenzyme binding [15]. This loop is absent in other MDR forms, including the *Amycolatopsis* enzyme. Hence, the general nature of nicotinoproteins is unclear and data for the *Amycolatopsis* nicotinoprotein ADH are essential. Its primary structure, modelled tertiary structure and deduced binding interactions are now reported. The data define this enzyme form, suggest yet another nicotinoprotein ADH type, and are of interest for evaluating general properties in nicotinoproteins.

Materials and methods

Protein analysis

Nicotinoprotein ADH was purified from the Gram-positive bacterium *A. methanolica* [8]. The protein was carboxymethylated in 6 M guanidinium chloride, 0.4 M Tris, pH 8.15, 2 mM EDTA by reduction with dithiothreitol and treatment with iodoacetate as described for other ADHs [9]. Buffer and excess reagents were removed by gel filtration (Sephadex G50; 4.6 × 250 mm) in 30% acetic acid. The carboxymethylated protein was cleaved in separate batches with *Achromobacter* Lys-specific protease (Waco), *Staphylococcus* Glu-specific protease (Boehringer), both at protease/substrate ratios of 1/10 for 4 h, *Pseudomonas* Asp-specific protease (Boehringer) at a ratio of 1/125 for 20 h, trypsin (Worthington) at a ratio of 1/25 for 4 h, and chymotrypsin (Sigma) at a ratio of 1/100 for 4 h, all at 37 °C in 0.1 M ammonium bicarbonate, pH 8.1, with up to 2.2 M urea for solubilization. Peptides obtained were separated by reverse phase HPLC on Vydac C_8 (2.1 mm × 250 mm), C_{18} (4.6 × 150 mm) or C_4 (4.6 × 250 mm) columns with a linear gradient of acetonitrile in aqueous 0.1% trifluoroacetic acid. Sequence degradations were performed on N-terminal sequencers (Applied Biosystems and MilliGene instruments) and on a C-terminal sequencer (Applied Biosystems 494C) allowing extended degradations [16]. Total compositions were determined by amino acid analysis after hydrolysis for 24 h at 110 °C with 6 M HCl/0.5% phenol. Peptide molecular masses were determined with Finnigan MALDI-TOF Lasermat 2000 and Micromass VG AutoSpec mass spectrometers.

Alignments, modelling and calculations

Sequence alignments and phylogenetic relationships were evaluated using the program CLUSTAL W [17] with bootstrap analysis [18]. Tree constructions were made in program TREEVIEW [19]. Molecular modelling of the primary structure determined was performed with the program ICM (version 2.7; Molsoft LLC) with the known structure of human class Iβ ADH (1hdx [20]) as template. In this procedure, aligned residues were tethered to the template structure and relaxed by energy refinements. Deletions and gaps were modelled by biased probability Monte Carlo simulation [21]. Conformation of each residue pair (class I versus the nicotinoprotein) was evaluated by overlaying the model with the Iβ structure. Pentafluorobenzyl alcohol or cyclohexanol and the coenzyme were coordinated at the active site in a substrate-like geometry as obtained from the corresponding crystal structures of the class I horse [22] and human [20] ADHs. The conformation of the coenzyme was taken from the template.

Results

Primary structure

The primary structure of nicotinoprotein ADH from *A. methanolica* was determined by amino acid sequence analysis of the intact carboxymethylated protein and of 82 constituent peptides obtained through five digests with proteolytic enzymes (fig. 1). The results gave overlapping fragments for all regions (fig. 1), and the peptides were also checked for mass consistency by mass spectrometry (table 1). The N terminus was not blocked, in contrast to that of many MDR ADHs [23]. Utilizing the peptide structures obtained, cloning of the corresponding cDNA was attempted. A full-length clone was never obtained, but segments corresponding to large parts of residues 83–204 were verified at the cDNA level. Combined, the sequencer and mass data establish a 371-residue polypeptide chain (fig. 1) with a mass of 38.97 kDa as the subunit of the nicotinoprotein ADH.

Alignment, modelling and active site

The sequence determined was submitted to molecular modelling using the program ICM with the MDR human class 1β ADH (1 hdx) structure as template. Results confirm the homology visible from alignments and show that the nicotinoprotein can be strictly modelled into the MDR ADH fold (fig. 2). Apart from the presence of seven short deviating loops corresponding to gaps and insertions (table 2), conformations between the human ADH structure and the nicotinoprotein model are closely similar (mean deviation of corresponding C_α atoms: 0.95 Å). The catalytic and structural zinc atoms and all their seven ligands of the mammalian ADH subunit are present at identical positions in the nicotinoprotein model (fig 2). This general agreement in fold and important residues strongly suggests that enzymatic mechanisms and active-site relationships are highly similar.

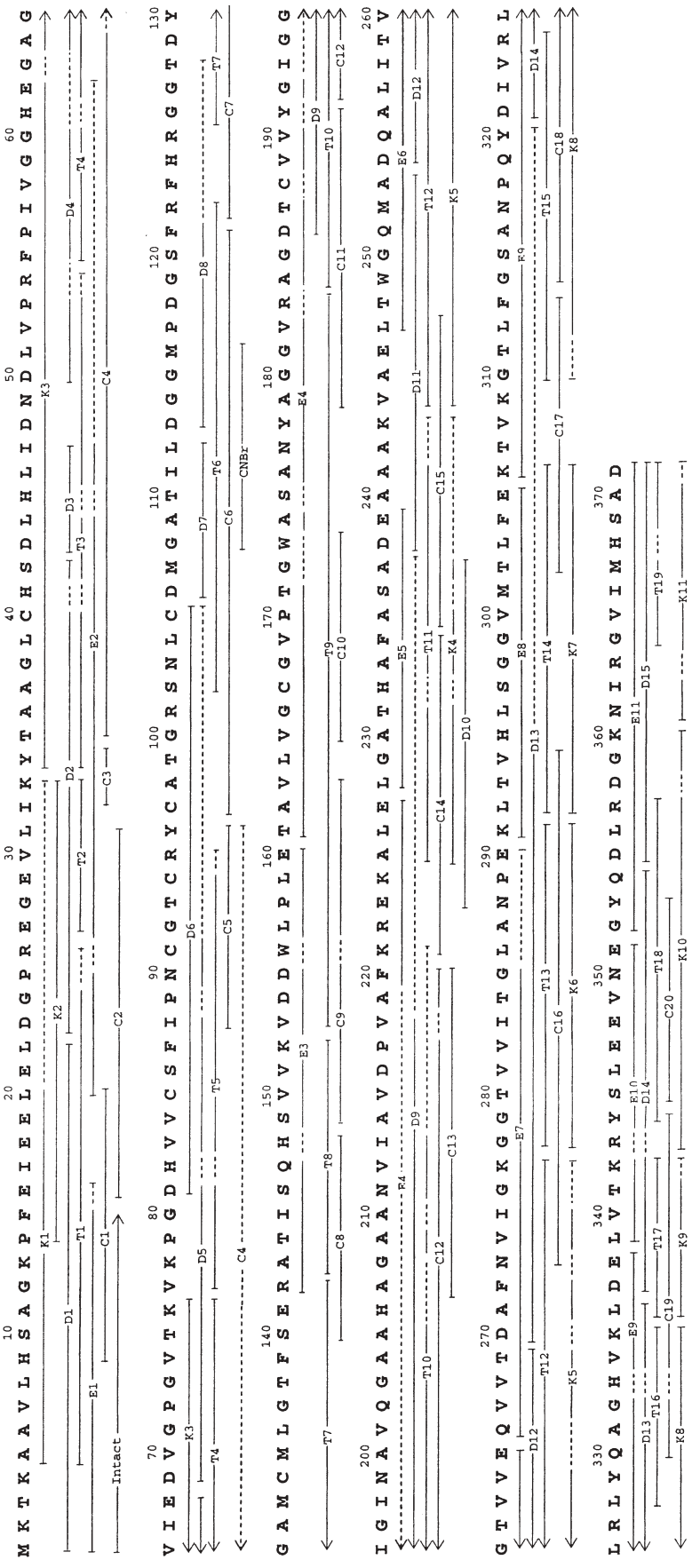

Figure 1. Primary structure of *Amycolatopsis methanolica* nicotinoprotein ADH, and positions of peptides analysed (consecutively numbered, with first letter indicating proteolytic enzyme used: T, trypsin; K, Lys-protease; D, Asp-protease; E, Glu-protease; C, chymotrypsin).

Table 1. Mass analyses of proteolytic peptides from nicotinoprotein ADH.

Peptide	Analyzed mass	Calculated mass
M1–L22	2442.8	2441.3
A5–R26	2380.3	2378.2
D23–S42	2174.4	2174.0
T35–Y96	6683.9	6685.2
Y34–K76	4496.0	4497.2
D50–E68	1963.1	1962.0
D69–C105	4144.9	4144.8
V77–R95	2206.7	2206.0
D81–C105	3011.7	3009.2
C97–F121	2606.9	2605.1
R122–Y130	1108.6	1108.5
G126–R142	1854.9	1853.8
R142–E160	2194.9	2193.2
A143–K152	1070.4	1069.6
V153–R183	3231.8	3231.6
A179–Y191	1326.3	1325.6
A184–K221	3624.7	3624.9
G192–F220	2630.2	2630.4
E223–A237	1517.4	1515.8
D238–A253	1691.1	1690.9
A233–L247	1464.2	1463.7
Q266–E290	2498.6	2499.3
D270–Y320	5295.0	5295.0
D270–L339	7172.0	7171.4
Q330–Y344	1757.4	1757.0
Y344–R357	1714.6	1714.8
G352–D371	2246.4	2245.1
M1–D371	38968.7	38967.7

Peptides shown are selected from figure 1, and defined by the identity and positional number of their first and last amino acid residue, respectively. Bottom line shows the values for the entire polypeptide chain. Analysis by MALDI-TOF mass spectrometry for most peptides, and by electrospray mass spectrometry for the entire protein chain and for the large peptides starting at position 270. The latter two peptides had oxidized Met301, adjusted for in the calculated mass.

Table 2. Structural alignment of the nicotinoprotein ADH with the human Iβ enzyme.

Loop		Sequence	Designation
1	Np:	NLC– – –DM	N103–M107
	1β:	NYCLKNDL	N109–L116
2	Np:	ATILDG	A109–G114
	1β:	NP– –RG	N118–G121
3	Np:	SAD– – –EAA	S236–A241
	1β:	PQDYKKPIQ	P243–Q251
4	Np:	QMADQ	Q251–Q255
	1β:	GV–DF	G261–F264
5	Np:	GTVVE	G261–E265
	1β:	GR–LD	G270–D273
6	Np:	LANPE	L286–E290
	1β:	VP–PA	V294–A297
7	Np:	LSGGV	L296–V300
	1β:	IN–PM	I303–M306

The alignment starts with Met1 of the nicotinoprotein corresponding to Ile7 of the human enzyme, and proceeds with direct continuity at all positions, except at seven loop regions, defined from the tertiary structure comparison of the nicotinoprotein model with the human structure (fig. 2), and ends with Phe374 of the human protein corresponding to His368 of the nicotinoprotein. This alignment also defines alignments of the nicotinoprotein to other MDR ADH forms (used in fig. 4), since human and horse class I ADH coalign and are used in reported alignments with other forms [cf. ref. 3]. Np, this nicotinoprotein; 1β, the human 1β form.

This finding made it meaningful to compare the residues at the positions lining the substrate pocket of the human enzyme (table 3). In the present alignment, based on the structural assignments, the nicotinoprotein residue corresponding to liver ADH position 116 differs from that quoted before [11, 12] because of a different gap assignment. Of 13 residues recognized at the active site of the conventional enzyme [24] (table 3), five are identical in the nicotinoprotein, six more are conservatively exchanged in a manner also seen in conventional ADHs, and the remaining two also do not alter charge relationships. Hence, one may conclude that the nicotinoprotein has a standard, largely hydrophobic ADH active site (table 3). Only two types of differences appear noticeable. One is the replacement of Leu141 in the conventional subunit with Cys in the nicotinoprotein, adding some polarity to the active site. The other is at the conventional ADH positions 115 and 116, which, although unchanged (Asp115) or conservatively changed (Leu116 to Met) in the nicotinoprotein (table 3), are part of a loop structure in the conventional enzyme that deviates in the nicotinoprotein structure because of preceding gap positions (table 2, fig. 2). Therefore, these two active-site residues contribute to a wider substrate-binding pocket at this site in the nicotinoprotein model.

Coenzyme binding

These relationships are relevant when evaluating the nicotinoprotein model to explain the tight NAD(H) binding in the nicotinoprotein. Three results are then noticeable. One is that considerable parts of the coenzyme binding in the conventional enzyme [20, 25] are also present in the nicotinoprotein (table 3). Furthermore, the coenzyme conformation from the mammalian class I template fits into the coenzyme-binding pocket with only minor deviations (fig 3). In particular, His41 of the nicotinoprotein pocket is capable of binding the nicotinamide oxygen like His47 in the conventional enzyme, Arg363 in the nicotinoprotein model has a conformation identical to that of Arg369 of the conventional enzyme and the interactions with the template nicotinamide phosphate are sustained in the nicotinoprotein model.

The second result is that alterations in two loop structures affect coenzyme binding and appear to tighten it in the nicotinoprotein model. Thus, a deviating loop in the nicotinoprotein starts at position 261 (fig. 3), and the shorter side chain of Thr262 compared with the corre-

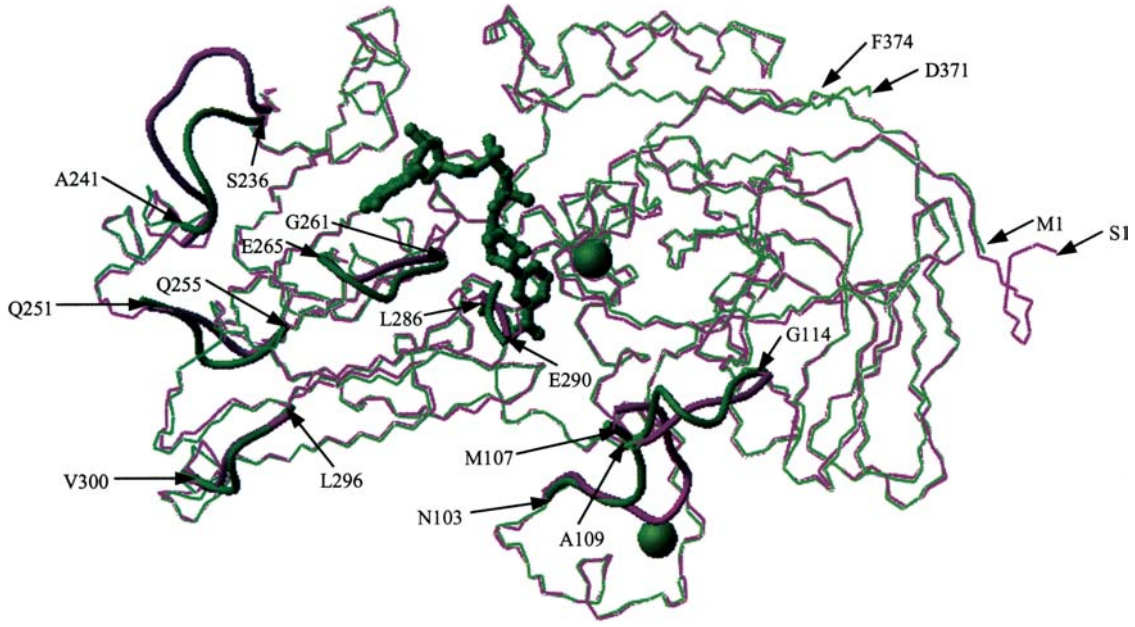

Figure 2. Overall conformational close agreement between the human 1β ADH structure (magenta) and the *Amycolatopsis* model (green). Only seven loop structures (shown in bold) deviate more because of gap positions from insertions/deletions.

Table 3. Comparison of functionally important residues in the currently analysed nicotinoprotein structure and the template structure of the human class Iβ ADH.

Substrate-binding pocket				Coenzyme-interacting residues				Residues withing a sphere of 3.8 Å around the coenzyme			
Np		Iβ		Np		Iβ		Np		Iβ	
Inner part				41	His	47	Arg	167	Cys	174	Cys
42	Ser	48	Thr	42	Ser	48	Thr	192	Gly	199	Gly
61	His	67	His	45	His	51	His	193	Ile	200	Leu
87	Phe	93	Phe	171	Thr	178	Thr	194	Gly	201	Gly
133	Met	140	Phe	196	Ile	203	Val	195	Gly	202	Gly
134	Cys	141	Leu					259	Thr	268	Val
Middle part				216	Asp	223	Asp	284	Thr	292	Val
51	Leu	57	Leu	217	Pro	224	Ile	310	Gly	316	Gly
106	Asp	115	Asp	221	Lys	228	Lys	311	Thr	317	Ala
107	Met	116	Leu	260	Val	269	Ile	313	Phe	319	Tyr
286	Leu	294	Val	262	Thr	271	Arg	258	Ile	267	(Glu)
312	Leu	318	Val	363	Arg	369	Arg	266	Gln	274	(Thr)
Outer part								286	Leu	294	(Val)
104	Leu	110	Tyr					288	Asn	–	–
300	Val	306	Met								
303	Leu	309	Leu								

The structures are those initially assigned for the horse class I ADH [24], a classification into three sets of active-site residues, directly coenzyme binding residues and residues within a sphere of 3.8 Å around the coenzyme now interpreted as being able to form additional interactions with the coenzyme (lower four Np residues), but with counterparts (within parentheses) less favourable for binding, or absent (–), in Iβ. Np, the nicotinoprotein ADH; Iβ, the human class Iβ form [assignments in the mammalian enzyme from refs 20, 24, 25].

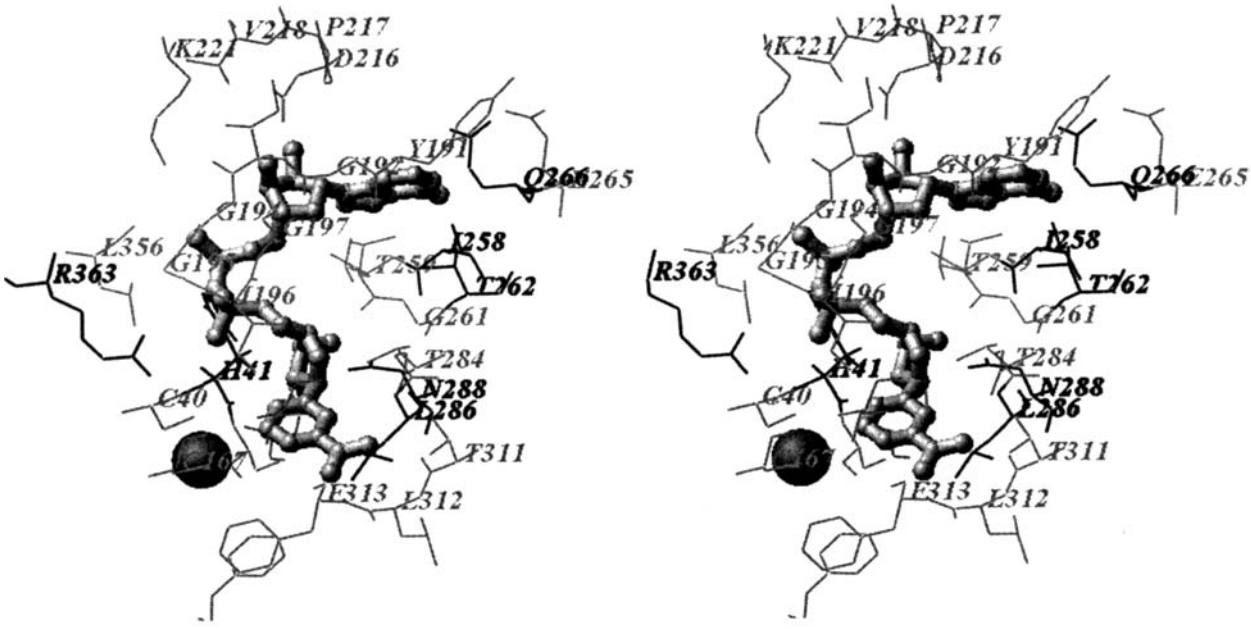

Figure 3. Three-dimensional relationships for the coenzyme (bold) bound to the *Amycolatopsis* model structure (grey), as deduced by docking the bound coenzyme from mammalian class I enzymes [20, 25] to the coenzyme site of the modelled bacterial enzyme. Residues indicated in black are those discussed in the text and differing most compared with the conventional enzyme.

sponding Arg271 in the conventional enzyme gives the coenzyme adenine ring enough space for a rotation of a few degrees (2–5° of its γ_A), lowering the adenine ring towards the active site. The other loop difference appears to be of even greater importance and may constitute the decisive difference in coenzyme binding. Thus, the segment comprising residues 292–298 in the conventional enzyme, critically involved in the conformational change required for coenzyme binding and release [22], is different in the nicotinoprotein model. There, the insertion of Asn288 alters the character of the entire loop due to its close proximity with the nicotinamide ribose. Nicotinoprotein Asn288 appears to be capable of additional hydrogen bonding with the nicotinamide ribose (fig. 3). In addition, this residue insertion in the nicotinoprotein may block the corresponding conformational change of this segment in the conventional enzyme. Insertion of Asn288 may therefore produce a substantial part of the nicotinoprotein nature by blocking both a critical loop movement in coenzyme binding/release and providing an extra H bond to the coenzyme.

Finally, the third result is that the positions of residues in a sphere of 3.8 Å around the coenzyme template of the nicotinoprotein model reveal the presence of coenzyme interactions additional to those in the conventional structure (table 3). Thus, in addition to Asn288 mentioned above, Gln266 in the nicotinoprotein is in the proximity of the adenine ring. The corresponding Thr274 side chain of the conventional enzyme is shorter and further away than Gln266 of the model. Furthermore, the exchange of conventional Glu267 to nicotinoprotein Ile258 gives an altered position and may provide further interactions with the coenzyme in the nicotinoprotein. A similar situation may apply to the exchange of conventional Val294 to nicotinoprotein Leu286.

In conclusion, the results show that the coenzyme interactions in the conventional MDR ADHs largely apply to the nicotinoprotein enzyme, but that additional residues give a few further interactions, two loop regions may tighten the binding and the crucial residue may be the inserted Asn288 in the nicotinoprotein. It may provide an extra H bond to the coenzyme and may negatively influence the conformational changes necessary for coenzyme movement during the enzyme reaction.

Discussion

The present analysis of nicotinoprotein ADH from *A. methanolica* defines this protein as an MDR enzyme and gives reasonable explanations for the strong coenzyme binding. Surprisingly, the protein is residuewise most closely similar to the class I vertebrate enzymes (38% residue identity) and to the mycothiol-dependent enzyme from the same bacterial species (31%). Presumably, the overall similarities with the mycothiol-dependent bacterial protein indicate a fairly close ancestral connection, while the larger similarities to the mammalian class I rather than class III enzymes may be derived from functional convergence. Construction of a

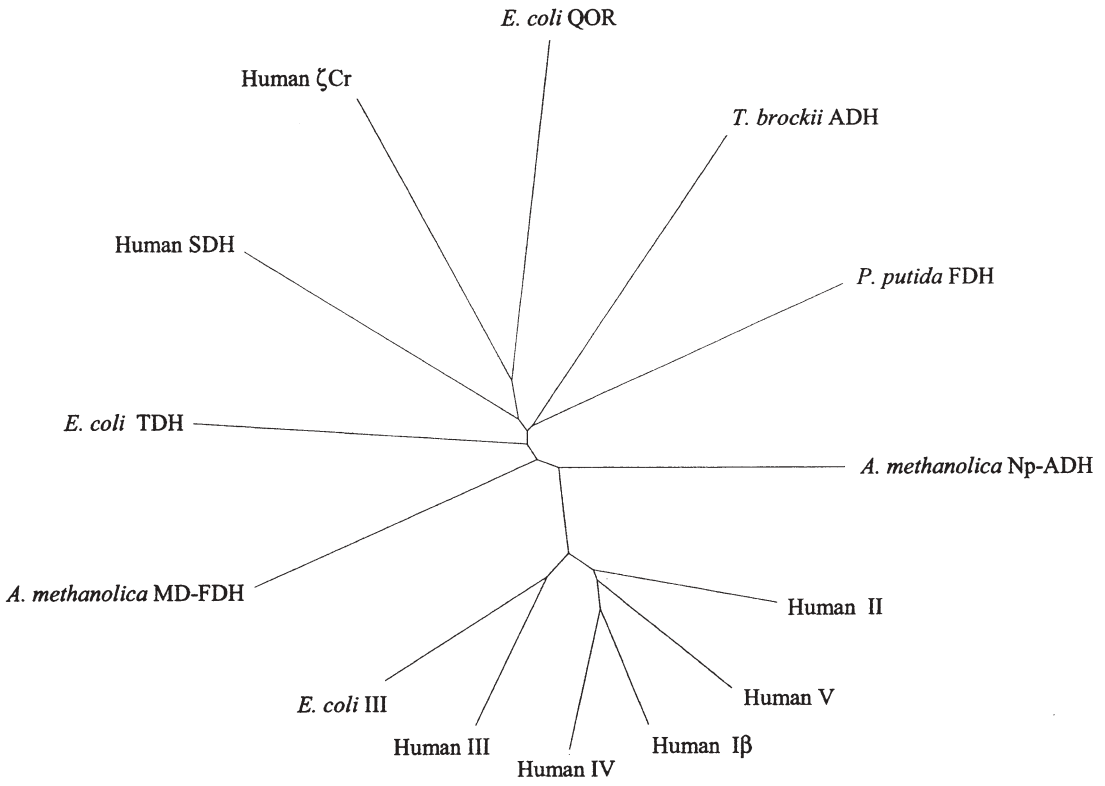

Figure 4. Unrooted phylogenetic tree relating major forms of MDR ADHs. As shown, the present protein (Np-ADH) is most closely positioned to the mycothiol-dependent ADH from the same species (MD-FDH), and more distantly related to all other forms of ADH, FADH (formaldehyde DH), TDH (threonine DH), SDH (sorbitol DH), QOR (quinone oxidoreductase) and ζ-Cr (ζ-crystallin).

phylogenetic tree from the present structure (fig. 4) supports this view and suggests the ancestral position of this nicotinoprotein to be most closely associated with that of the mycothiol form, far from those of the classes of conventional MDR ADHs. Significantly, the results also show that nicotinoproteins are not a structurally homogeneous entity. The present enzyme is an MDR form, other ADH-related nicotinoproteins have been shown to be SDR forms [13] or MDR forms with a loop insertion elsewhere [15]. Independent of final details on further forms, the finding of nicotinoproteins of three types shows that the nicotinoprotein property has been acquired repeatedly in nature and thus by itself does not indicate ancestral connections, but merely structural acquirements of strong coenzyme binding.

Regarding the tight coenzyme binding, the present results reveal structural explanations. Apparently, at least three factors are important for the tight binding. One is the presence of the general coenzyme-binding pocket of the conventional MDR ADH and its residues in coenzyme interactions (table 3). Another is the presence of additional coenzyme interactions with further residues due to both individual residue replacements and loop alterations derived from insertions/gaps. A third, and apparently the key factor, appears to be additional hydrogen bonding to the coenzyme, and in particular an interference with the protein conformational changes necessary for coenzyme movement in the conventional ADHs. Although the results, combined with those of previous data [13–15], suggest that increased coenzyme binding may still be obtained in different manners, one common mode may still exist in the sense that alterations in loop structures appear to mediate the increased SDR and MDR coenzyme binding [see refs 13, 15] (fig. 2). This may suggest loop alterations as a general mode for the differential acquirement of coenzyme interactions in dehydrogenases.

Acknowledgements. We are grateful to Drs B. Persson and W. Griffiths, Karolinska Institutet, and Dr S. de Vries, Delft University of Technology, for advice and to I. Byman, E. Cederlund and C. Palmberg for assistance. Support from the Swedish Research Council (project 03X-3532), Karolinska Institutet, and the NWO-Chemische Wetenschappen is gratefully acknowledged.

1 Nordling E., Persson B. and Jörnvall H. (2002) Differential multiplicity of MDR alcohol dehydrogenases: enzyme genes in the human genome versus those in organisms initially studied. Cell. Mol. Life Sci. **59:** 1070–1075

2 Jörnvall H., Nordling E. and Persson B. (2003) Multiplicity of eukaryotic ADH and other MDR forms. Chem. Biol. Interact. **143–144:** 255–261

3 Nordling E., Jörnvall H. and Persson B. (2002) Medium-chain dehydrogenases/reductases (MDR): family characterizations including genome comparisons and active site modelling. Eur. J. Biochem. **269:** 4267–4276
4 Kallberg Y., Oppermann U., Jörnvall H. and Persson B. (2002) Short-chain dehydrogenases/reductases (SDRs): coenzyme-based functional assignments in completed genomes. Eur. J. Biochem. **269:** 4409–4417
5 Crosas B., Cederlund E., Torres D., Jörnvall H., Farrés J. and Parés X. (2001) A vertebrate aldo-keto reductase active with retinoids and ethanol. J. Biol. Chem. **276:** 19132–19140
6 Inoue T., Sunagawa M., Mori A., Imai C., Fukuda M., Takagi M. et al. (1989) Cloning and sequencing of the gene encoding the 72-kilodalton dehydrogenase subunit of alcohol dehydrogenase from *Acetobacter aceti*. J. Bacteriol. **171:** 3115– 3122
7 Scopes R. K. (1983) An iron-activated alcohol dehydrogenase. FEBS Lett. **156:** 303–306
8 van Ophem P. W, van Beeumen J. and Duine J. A. (1993) Nicotinoprotein [NAD(P)-containing] alcohol/aldehyde oxidoreductases. Eur. J. Biochem. **212:** 819–826
9 Norin A., van Ophem P. W., Piersma S. R., Persson B., Duine J. A. and Jörnvall H. (1997) Mycothiol-dependent formaldehyde dehydrogenase, a prokaryotic medium-chain dehydrogenase/reductase, phylogenetically links different eukaryotic alcohol dehydrogenases. Eur. J. Biochem. **248:** 282–289
10 Piersma S. R., Visser A. J. W. G., de Vries S. and Duine J. A. (1998) Optical spectroscopy of nicotinoprotein alcohol dehydrogenase from *Amycolatopsis methanolica*: a comparison with horse liver alcohol dehydrogenase and UDP-galactose epimerase. Biochemistry **37:** 3068–3077
11 Piersma S. R. (1998) On the structure and catalytic mechanism of nicotinoprotein alcohol dehydrogenases from *Amycolatopsis methanolica*. PhD thesis, Delft University of Technology
12 Schenkels P. and Duine J. A. (2000) Nicotinoprotein (NADH-containing) alcohol dehydrogenase from *Rhodococcus erythropolis* DSM 1069: an efficient catalyst for coenzyme-independent oxidation of a broad spectrum of alcohols and the interconversion of alcohols and aldehydes. Microbiology **146:** 775–785
13 Thoden J. B., Frey P. A. and Holden H. M. (1996) Crystal structures of the oxidized and reduced forms of UDP-galactose 4-epimerase isolated from *Escherichia coli*. Biochemistry **35:** 2557–2566
14 Kingston R. L., Scopes R. K. and Baker E. N. (1996) The structure of glucose-fructose oxidoreductase from *Zymomonas mobilis*: an osmoprotective periplasmic enzyme containing non-dissociable NADP. Structure **4:** 1413–1428
15 Tanaka N., Kusakabe Y., Ito K., Yoshimoto T. and Nakamura K. T. (2002) Crystal structure of formaldehyde dehydrogenase from *Pseudomonas putida*: the structural origin of the tightly bound cofactor in nicotinoprotein dehydrogenases. J. Mol. Biol. **324:** 519–533
16 Bergman T., Cederlund E. and Jörnvall H. (2001) Chemical C-terminal protein sequence analysis: improved sensitivity, length of degradation, proline passage, and combination with Edman degradation. Anal. Biochem. **290:** 74–82
17 Thompson J. D., Higgins D. G. and Gibson T. J. (1994) CLUSTAL W: improving the sensitivity of progressive multiple sequence alignment through sequence weighting, position-specific gap penalties and weight matrix choice. Nucleic Acids Res. **22:** 4673–4680
18 Felsenstein J. (1985) Confidence limits on phylogenies: an approach using the bootstrap. Evolution **39:** 783–791
19 Page R. D. M. (1996) TREEVIEW: an application to display phylogenetic trees on personal computers. Comp. Appl. Biosci. **12:** 357–358
20 Hurley T. D., Bosron W. F., Stone C. L. and Amzel L. M. (1994) Structures of three human beta alcohol dehydrogenase variants: correlation with their functional differences. J. Mol. Biol. **239:** 415–429
21 Abagyan R. A. and Totrov M. M. (1994) Biased probability Monte Carlo conformational searches and electrostatic calculations for peptides and proteins. J. Mol. Biol. **235:** 983–1002
22 Ramaswamy S., Eklund H. and Plapp B. V. (1994) Structures of horse liver alcohol dehydrogenase complexed with NAD^+ and substituted benzyl alcohols. Biochemistry **33:** 5230–5237
23 Hjelmqvist L., Hackett M., Shafqat J., Danielsson O., Iida J., Hendrickson R. C. et al. (1995) Multiplicity of N-terminal structures of medium-chain alcohol dehydrogenases: mass-spectrometric analysis of plant, lower vertebrate and higher vertebrate class I, II, and III forms of the enzyme. FEBS Lett. **367:** 237–240
24 Eklund H., Müller-Wille P., Horjales E., Futer O., Holmquist B., Vallee B. L. et al. (1990) Comparison of three classes of human liver alcohol dehydrogenase: emphasis on different substrate binding pockets. Eur. J. Biochem. **193:** 303–310
25 Eklund H., Samama J.-P. and Jones T. A. (1984) Crystallographic investigations of nicotinamide adenine dinucleotide binding to horse liver alcohol dehydrogenase. Biochemistry **23:** 5982–5996